BMC Oral Health

RESEARCH

Open Access

Salivary transcriptomic profile reveals biomarker candidates for early detection of occlusal dysesthesia: a case–control study

Yuan Li[1], Yanfeng Kang[1], Yaojun Zhang[1], Jingwen Liu[1], Siyi Mo[1], Yang Xue[1], Chao Yuan[2], Kaiyuan Fu[3], Qiufei Xie[1], Xiaoxiang Xu[1*] and Ye Cao[1*]

Abstract

Background Occlusal dysesthesia (OD) is a rare and highly intractable condition, with no established objective indicators for early detection. This study aimed to analyze the salivary transcriptomic profiles of OD patients and healthy controls to explore potential biomarkers for early OD detection.

Methods Saliva samples were collected from 11 OD patients and 11 age- and gender-matched healthy controls, then processed for RNA sequencing. Differential gene expression and functional enrichment analyses were performed. Selected candidate mRNA markers were validated using real-time polymerase chain reaction (PCR). Firth's penalized logistic regression was applied to assess the association between OD and each candidate mRNA marker. The diagnostic utility of these genes was evaluated using Receiver Operating Characteristic (ROC) curve analysis.

Results The total number of identified mRNAs in saliva was 5353 ± 2214 in OD patients and 5075 ± 1482 in controls. A total of 595 significantly differentially expressed mRNAs were identified, including 320 up-regulated and 275 down-regulated. Based on the differential expression profile, 16 mRNAs were selected as potential biomarker candidates, of which 15 were confirmed by real-time PCR. Regression analysis revealed that *OSTC*, *HES1*, *HINT2*, *VTI1B*, *SNX6*, and *PGRMC1* were associated with increased OD risk, whereas *AZGP1*, *CLDN3*, *SLC27A4*, *RRAS*, *GAS1*, *TAGLN*, *CTTNBP2NL*, and *PLAC9* were associated with reduced risk. Regarding diagnostic performance, the top three single-gene predictors for OD detection were *CLDN3*, *RRAS* and *PGRMC1* (corrected AUC > 0.90), and the top three two-gene panels were *CLDN3* + *SNX6*, *CLDN3* + *PGRMC1*, and *AZGP1* + *SNX6* (corrected AUC > 0.98). Adding a third gene did not improve diagnostic performance compared with the two-gene panels.

Conclusion This study provides the first characterization of the salivary transcriptomic profile in OD patients, and identifies potential salivary mRNA biomarker candidates associated with OD.

Trial registration Chinese Clinical Trial Registry, ChiCTR2000040994; Registered on 16 December 2020.

Keywords Biomarker, Occlusal dysesthesia, RNA sequencing, Saliva, Transcriptome

*Correspondence:
Xiaoxiang Xu
xiaoxiang86@bjmu.edu.cn
Ye Cao
ye.cao@bjmu.edu.cn

Full list of author information is available at the end of the article

© The Author(s) 2026. **Open Access** This article is licensed under a Creative Commons Attribution 4.0 International License, which permits use, sharing, adaptation, distribution and reproduction in any medium or format, as long as you give appropriate credit to the original author(s) and the source, provide a link to the Creative Commons licence, and indicate if changes were made. The images or other third party material in this article are included in the article's Creative Commons licence, unless indicated otherwise in a credit line to the material. If material is not included in the article's Creative Commons licence and your intended use is not permitted by statutory regulation or exceeds the permitted use, you will need to obtain permission directly from the copyright holder. To view a copy of this licence, visit http://creativecommons.org/licenses/by/4.0/.

Background

Occlusal dysesthesia (OD) is a rare and highly intractable condition, historically described by various terms, including phantom bite syndrome, occlusal hyperawareness, occlusal neurosis, occlusal discomfort syndrome, or oral cenesthopathy [1–3]. Its primary characteristics include persistent abnormal sensations related to occlusion, such as discomfortable occlusion, disordered bite, incorrect tooth or mandibular positioning, and even aberrant sensations like teeth moving throughout the body [4–6]. However, objective evidence supporting these symptoms cannot be identified through current clinical examination, and all interventions targeting occlusion are ineffective or may exacerbate the condition [7–11]. Many OD patients endure severe distress due to persistent symptoms and unsuccessful treatments, with some reports indicating case of suicide [12]. The pathogenesis of OD remains unclear, although prevailing perspectives classify it as a mental disorder with somatic symptoms associated with central nervous system (CNS) dysfunction [13, 14]. Irreversible dental treatments should be avoided; instead, patient education, cognitive behavior therapy, and psychiatric medications are recommended [13, 14]. Diagnosis of OD currently relies primarily on clinical symptoms and patient history, particularly a history of multiple ineffective dental treatments. Delayed diagnosis worsens patient outcomes, consumes medical resources, and can strain the doctor-patient relationship. Since OD patients typically first seek care in dental clinics, developing simple, convenient, and objective examination methods for early OD detection is clinically important for guiding appropriate treatment or referral decisions, benefiting both patients and clinicians. Several attempts have been made to identify objective indicators for OD diagnosis. Some studies compared the occlusal thickness discrimination function between OD patients and healthy individuals, finding no differences [15, 16]. Another study evaluated frontal lobe cortical activity during active grinding using functional near-infrared spectroscopy and reported significant differences in deoxyhemoglobin signals in OD patients [17]. However, this method requires specialized equipment and is not feasible as a widespread screening tool, particularly in dental settings.

In recent years, the rapid advancement of analytical technologies has greatly facilitated the identification of biomarkers for specific diseases in various body fluids. Saliva, in particular, has emerged as a popular sample choice due to its non-invasive, convenient, and safe collection methods, offering promising prospects for disease diagnosis, monitoring, and prediction [18, 19]. Substances present in serum can enter saliva through passive diffusion, active transport, or extracellular ultrafiltration mechanisms [20], allowing saliva to reflect changes in the physiological functions of the entire body to some extent [21]. With the continued progress in high-throughput omics technologies, salivomics has gained increasing attention for saliva analysis, involving methodologies such as proteomics, transcriptomics, metabolomics, and microbiomics [22]. Transcriptomics, the study of gene transcripts and their quantities in a specific sample, provides high informativeness and discriminability. It not only confirms the presence of genes but also offers insights into their expression status, revealing the molecular composition of specific tissues under certain conditions, and thereby reflecting the organism's diverse physiological states and responses to pathological changes [23]. Numerous studies have confirmed the presence of thousands of human messenger ribonucleic acid (mRNA) molecules in saliva that can be extracted and detected [24, 25]. Notably, the slow degradation rate of salivary RNA suggests a mechanism that facilitates the stable existence of RNA in saliva [26], making salivary transcriptomics a promising tool for disease screening, diagnosis, and prognostic analysis. Specific mRNA molecules in saliva have been identified as potential biomarkers for various diseases, including oral diseases such as Sjögren's syndrome [27], oral cancer [28, 29], and periodontitis [30], as well as systemic diseases such as pancreatic cancer [31], gastric cancer [32], breast cancer [33], lung cancer [34], and ovarian cancer [35]. However, the salivary transcriptomic profile of patients with OD remains unexplored. This study aims to define the salivary transcriptomic characteristics of OD patients and explore potential biomarkers for early OD detection.

Methods

Study design

This study was designed as an observational case–control study. The protocol was approved by the Institutional Review Board of the Peking University School and Hospital of Stomatology (PKUSSIRB-202054059). OD patients were recruited between 2021 and 2023 from the Department of Prosthodontics and the Center for Temporomandibular Disorders and Orofacial Pain at Peking University School and Hospital of Stomatology, provided they met the inclusion criteria based on the clinical diagnostic principles for OD [14]. Age- and gender-matched healthy controls were enrolled at a 1:1 ratio, and were required to meet the following criteria: (1) no persistent pain throughout the body lasting longer than one week in the past six months; (2) natural or restored dentition without significant occlusal abnormalities; and (3) good oral hygiene. All participants received detailed information about the study procedures, and written consent was obtained. The participant recruitment flow is shown in Supplementary Fig. 1. All data were anonymized prior to analysis. The inclusion criteria for OD were: (1) core symptoms persisting for more than six months, including

discomfort and abnormalities in occlusion; (2) a notable discrepancy between reported symptom severity and objective examination findings, or the presence of unexplained symptoms; and (3) a history of multiple ineffective occlusal treatments. The exclusion criteria included: (1) uncontrolled diabetes, hypertension, or other severe systemic diseases; (2) prolonged use of non-therapeutic medications; and (3) primary complaints of orofacial pain, or alignment with pain diagnoses in temporomandibular disorders.

Trial registration and protocol amendments

This study was conducted as a predefined substudy of a registered clinical trial (Chinese Clinical Trial Registry: ChiCTR2000040994; Registered on 16 December 2020). The parent trial aimed to delineate the clinical characteristics and gene expression profile in the peripheral blood of patients with OD and chronic orofacial pain, compared with matched controls. The present study reports prespecified secondary outcomes from one experimental arm and its matched control group. A sample size of 15 was determined based on the expected number of OD patients at our institutions during the study period. At the end, 11 patients were enrolled due to the rare nature of OD. During the study, the sampling procedure was amended to collect saliva samples instead of blood, considering patient safety, non-invasiveness, improved acceptability, and validation data demonstrating reliable detection performance with saliva. This modification affected only the collection method and did not alter the scientific objectives or the interpretability of the findings. This change was approved by the Institutional Review Board of Peking University Hospital of Stomatology (PKUSSIRB-202054059a) on 29 January 2021 and was subsequently updated in the registry. The present study adheres to the updated registered protocol.

Sample collection

Saliva samples were collected between 9:00 and 10:00 a.m. in accordance with previously published protocols [36–38]. Participants refrained from eating, drinking, smoking, and oral hygiene cleaning for at least one hour prior to collection. Before sampling, the oral cavity was thoroughly rinsed with deionized water to remove residual saliva. Sterile, defatted cotton rolls from saliva collection tubes (Salivette®, SARSTEDT, Germany) were placed under the tongue to collect naturally secreted saliva. Once saturated, the cotton rolls were removed and placed into the collection tubes. The saliva collection tubes were centrifugation at 3000 rpm and 4 °C for 5 min. The inner tube and cotton roll were discarded, and the supernatant from the outer tube was stored at −80 °C for subsequent sequencing analyses.

RNA extraction, library construction and sequencing procedures

Total RNA from saliva samples was extracted using the RNeasy Mini Kit (Qiagen, 217,184) following the manufacturer's instructions. RNA integrity was assessed using an Agilent 4200 TapeStation. Qualified total RNA was further purified with the RNAClean XP Kit (Beckman Coulter, A63987) and the RNase-Free DNase Set (Qiagen, 79,254). RNA purity was evaluated using the ThermoFisher NanoDrop™ 2000 spectrophotometer. Purified RNA was then used for library construction with the Illumina TruSeq® Stranded Total RNA Library Preparation Kit (Illumina, 20,020,598). The constructed library was quantified using the ThermoFisher Qubit® 2.0 Fluorometer and validated with the Agilent 4200 bioanalyzer to assess insert size and concentration. Clusters were generated by cBot with the library diluted to 10 pM, followed by sequencing using the Illumina NovaSeq 6000 system. These procedures were conducted at Shanghai Biotechnology Corporation.

Processing and analysis of RNA sequencing data

Raw sequencing reads were subjected to quality assessment, including evaluation of per-base sequencing quality scores (Q-scores) and nucleotide composition. Adapter sequences and low-quality bases were trimmed using Seqtk (version 1.3). Reads were filtered to remove those with 3'-end bases having a Q-score below 20 (error rate < 0.01) and those shorter than 25 bp after trimming. Ribosomal RNA (rRNA) reads were removed by aligning to a species-specific rRNA database. The remaining high-quality, rRNA-depleted reads were aligned to the human GRCh38 reference genome using the splice-aware aligner HISAT2 (version 2.0.4) with default parameters, generating BAM format alignment files [39]. Gene abundance across all samples was quantified as the fraction of total (FOT) gene counts. The classes and cellular distribution of proteins encoded by the identified salivary genes were further investigated using the PANTHER knowledgebase (v18.0, https://pantherdb.org/) [40]. Stringtie (version 1.3.0) [41, 42] was employed to calculate Fragments Per Kilobase of exon model per Million mapped reads (FPKM) values based on a reference annotation. Differentially expressed genes were identified using edgeR (version 3.38.0) [43], with significance determined by the false discovery rate (FDR) [44]. The filtering criteria used were an FDR ≤ 0.05 and a fold-change ≥ 2. Functional enrichment analysis of these differentially expressed genes was performed using Metascape (https://metascape.org/) [45] with gene sets from the Gene Ontology (GO). Potential biomarker candidates were selected from the differential genes based on the following criteria: (1) FPKM > 10 for at least six individuals in either the case or control group; (2) |log2FC| > 2.5;

and (3) Total consistency score > 0. The consistency score for each gene was determined by assessing the direction of change in gene expression for individual paired case–control samples, relative to the overall expression trend between the two groups. Consistency scores were assigned as follows: 1 for uniform change, −1 for no change, and −2 for reverse change. The total consistency score for each gene was calculated as the sum of individual consistency scores across all case–control pairs.

Real-time polymerase chain reaction (PCR)

To verify differential expression of selected candidate mRNAs between OD patients and controls, real-time PCR was performed using the same residual salivary samples collected from the participants. Total RNA was isolated from the samples using Trizol reagent (Invitrogen, CA, US) and then converted into cDNA with SuperScriptTM III Reverse Transcriptase (Invitrogen). β-actin was used as the housekeeping gene for internal standardization. Specific primers for target and the reference genes were designed and listed in Supplementary Table 1. Real-time PCR was conducted using the QuantStudioTM 5 System (Applied Biosystems, CA, US) with Arraystar SYBR® Real-time PCR Master Mix, following the manufacturer's instructions. The cycling conditions were: initial denaturation at 95 °C for 10 min, followed by 40 cycles of 95 °C for 10 s and 60 °C for 1 min. Data were exported to Excel and analyzed using the $2^{-\Delta\Delta CT}$ method.

Statistical analysis

Continuous data were expressed as mean ± SD, while categorical data were presented as counts and percentages. Statistical analyses were performed using R (version 4.2.3). The normality of the data was verified with the Shapiro–Wilk test. The Student's t-test, Kruskal–Wallis test, and Fisher's exact probability test were employed as appropriate. To examine the association between OD and the expression of each candidate mRNA biomarker (△Ct values), Firth's penalized logistic regression were used, which incorporates a Jeffreys prior penalty to the log-likelihood and effectively resolves issues of quasi-complete separation and monotone likelihood often encountered in small sample sizes. Four logistic models were constructed: (1) unadjusted; (2) adjusted for age; (3) adjusted for gender; and (4) adjusted for both age and gender. The diagnostic utility of the genes was assessed using Receiver Operating Characteristic (ROC) curve analysis. The apparent Area Under the Curve (AUC) with 95% confidence intervals, and the corresponding sensitivity and specificity calculated by maximizing the Youden index were reported. To mitigate the overfitting risks inherent in small sample sizes, rigorous internal validations were applied through a 1000-resample Bootstrap optimism correction. The "Optimism-Corrected AUC" was utilized as the primary metric for true diagnostic discrimination. Finally, to explore whether a combination of biomarkers could yield incremental diagnostic value without violating the Events-Per-Variable statistical limits, exhaustive best-subset selection was performed for all 2-gene and 3-gene combinations. The best-performing parsimonious multi-maker panels were compared with the single-gene model. This study did not contain missing data. A significance level of $p < 0.05$ was applied.

Table 1 Demographic characteristics of the participants

Group	Age (Mean ± SD, y)	Male (n, %)	Female (n, %)
OD	46.73 ± 8.98	4 (36.4%)	7 (63.6%)
Control	45.55 ± 11.14	4 (36.4%)	7 (63.6%)

OD Occlusal dysesthesia, *SD* Standard deviation, *y* year

Results

Clinical characteristics of the study participants

A total of 11 patients with OD were included in this study. Age- and gender-matched controls relative to OD patients were enrolled. The demographic characteristics of the participants were presented in Table 1. No significant differences were observed between the two groups with respect to age or gender ($p > 0.05$). Detailed clinical characteristics of the OD patients are provided in Supplementary Table 2.

Overview of transcriptomic profiles in saliva

RNA sequencing analysis of saliva samples demonstrated high sequencing quality and balanced base composition. The detected reads were successfully mapped to multiple genomic regions, including exons, splicing sites, introns, non-coding regions, and intergenic regions. The mapping ratios for each region are shown in Fig. 1A: Gene region (0.868 ± 0.068), exon region (0.213 ± 0.129), splicing site region (0.046 ± 0.029), intron region (0.221 ± 0.084), non-coding region (0.433 ± 0.172), and intergenic region (0.132 ± 0.068). No significant difference in the region distribution of mapped reads was observed between the case and control groups ($p = 0.9217$).

The total number of identified genes in saliva samples from patients and controls were 5353 ± 2214 and 5075 ± 1482, respectively, with no significant difference between the groups ($p = 0.7331$) (Fig. 1B). The abundance of each identified gene in total salivary samples was quantified using the fraction of total (FOT), as shown in the rank plot of FOT values for all identified genes (Fig. 1C). The ten most abundant genes, including *RN7SL2*, *RN7SL1*, *MT-RNR2*, *MALAT1*, *NEAT1*, *MT-CO1*, *RN7SL4P*, *AL162581.1*, *S100A9*, and *PPL*, collectively accounted for 23.3% of the total gene abundance.

The classes and cellular distribution of proteins encoded by salivary mRNAs were analyzed using the PANTHER knowledgebase [40]. Among the 15,519

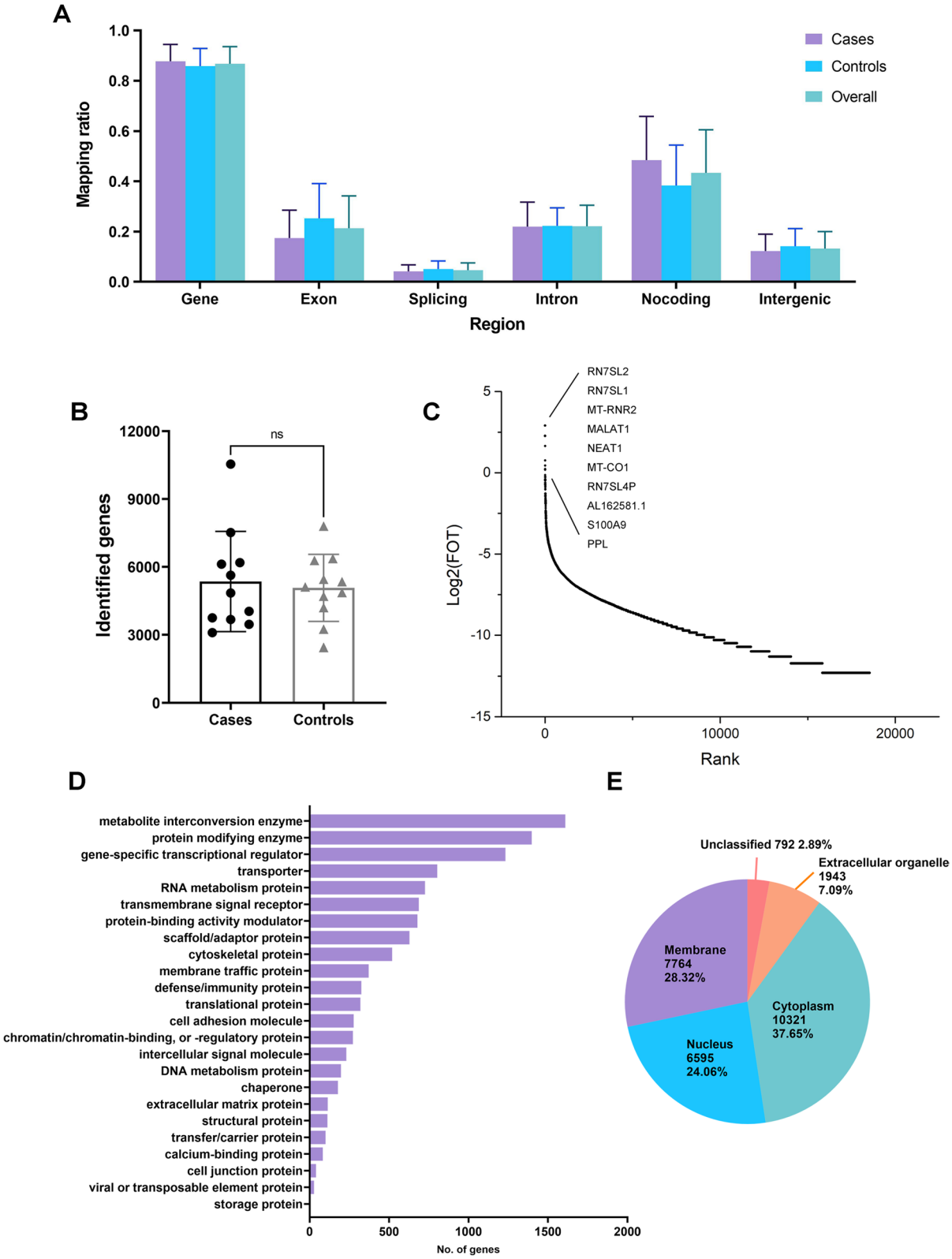

Fig. 1 Overview of transcriptomic profiles in saliva. **A** The mapping ratio of detected reads mapped to different gene regions (including exons, splicing sites, introns and non-coding regions) and intergenic regions through RNA sequencing in saliva of cases and controls. **B** Total number of identified genes in saliva of cases and controls. **C** The rank of overall abundance of each gene detected in saliva. **D** The classes of proteins encoded by the salivary transcriptome. **E** The cellular distribution of proteins encoded by the salivary transcriptome

protein-coding genes identified in saliva, 24 protein classes were annotated, while 4587 proteins remained unclassified. The ten largest protein classes included metabolite interconversion enzymes, protein modifying enzymes, gene-specific transcriptional regulators, transporters, RNA metabolism proteins, transmembrane signal receptors, protein-binding activity modulators, scaffold/adaptor proteins, cytoskeletal proteins, and membrane traffic proteins (Fig. 1D). Cellular component analysis indicated that 24.06% (6595), 28.32% (7764), and 37.65% (10,321) of proteins were localized to the nucleus, membrane, and cytoplasm, respectively. In addition, 7.09% (1943) of proteins were distributed extracellularly, whereas 2.89% (792) remained unclassified (Fig. 1E).

Differential expression and functional enrichment analysis

Differential expression analysis of the salivary transcriptome was conducted by comparing patients to controls, revealing 595 significantly differentially expressed mRNAs, with 320 up-regulated and 275 down-regulated (Fig. 2A). Metascape analysis [45] identified 692 significantly enriched GO biological process (BP) terms for up-regulated pathways, predominantly associated with localization, metabolic process, responses to stimuli, immune system process, developmental process, cellular process, and regulation of biological process. In contrast, 310 significantly enriched GO BP terms were identified for down-regulated pathways, primarily linked to developmental process, metabolic process, and cellular process (Fig. 2B). The top 10 enriched up-regulated GO BP terms included mitotic cell cycle, cell division, mitotic cell cycle process, endosomal transport, organelle localization, vesicle organization, import into cell, endocytosis, regulation of cell morphogenesis, and regulation of cell shape (Fig. 2C). A subset of representative up-regulated GO BP terms was visualized in an interaction network (Fig. 2D). The top 10 enriched down-regulated GO BP terms comprised complement activation, antibacterial humoral response, humoral immune response mediated by circulating immunoglobulin, supramolecular fiber organization, humoral immune response, cell–cell adhesion, actomyosin structure organization, antimicrobial humoral response, myofibril assembly, and cell–cell adhesion via plasma-membrane adhesion molecules (Fig. 2E). The relationships among the down-regulated BP terms were illustrated in Fig. 2F.

Determination of differential mRNAs as potential biomarker candidates

A total of 16 differential genes were identified as potential biomarker candidates based on the specific criteria outlined in the Methods section. Detailed information on these 16 mRNA candidates is provided in Supplementary Table 3. Heatmaps illustrating the expression of each mRNA candidate in all cases and controls are presented in Fig. 3A. Metascape analysis [45] was conducted to explore enriched functional pathways for these 16 candidate genes, resulting in the enrichment of 13 GO BP pathways for 11 genes, as shown in Fig. 3B. The interaction relationships among these GO BP terms are displayed in Fig. 3C.

Verification of candidate genes through real-time PCR

The expression of the 16 candidate genes was verified using real-time PCR. The results revealed that in the case group, six genes exhibited significant up-regulation: *OSTC* ($p = 0.0083$), *HES1* ($p = 0.0019$), *HINT2* ($p = 0.0004$), *SNX6* ($p = 0.0022$), *VTI1B* ($p = 0.001$), and *PGRMC1* ($p < 0.0001$). Additionally, nine genes were significantly down-regulated: *AZGP1* ($p < 0.0001$), *CLDN3* ($p < 0.0001$), *CTTNBP2NL* ($p = 0.0019$), *GAS1* ($p = 0.001$), *PLAC9* ($p = 0.002$), *RRAS* ($p < 0.0001$), *SLC27A4* ($p = 0.0002$), *TAGLN* ($p = 0.0017$), and *LTF* ($p = 0.0334$) (Fig. 4), compared to the control group. No significant difference in *CFD* expression was detected ($p = 0.094$).

Association of candidate salivary gene expression with OD

Using Firth's penalized regression, 14 gene expressions were identified as significantly associated with OD, which were presented in Table 2. An odds ratio (OR) > 1 indicates a reduced risk of OD, while an OR < 1 indicates an increased risk, as lower ΔCt values correspond to higher expression levels. In the unadjusted model, *AZGP1*, *CLDN3*, *SLC27A4*, *RRAS*, *GAS1*, *TAGLN*, *CTTNBP2NL*, and *PLAC9* were significantly associated with reduced OD risk, while *OSTC*, *HES1*, *HINT2*, *VTI1B*, *SNX6*, and *PGRMC1* were associated with increased risk. The association of *LTF* expression with OD was nonsignificant. These associations remained consistent after adjusting for age, gender, and both age and gender.

Diagnostic performance of single-marker models and parsimonious multi-marker panel

To establish a baseline for diagnostic utility, the performance of individual genes was initially evaluated. *CLDN3* emerged as the most potent single biomarker candidate for OD detection. Even after Bootstrap optimism correction, *CLDN3* alone achieved an outstanding AUC of 0.91, yielding a sensitivity of 100% and a specificity of 91%. Other notable single-gene predictors included *RRAS* and *PGRMC1* (optimism-corrected AUC = 0.90), indicating profound baseline transcriptomic alterations in OD patients. To determine whether a multi-marker strategy could capture complementary diagnostic information while avoiding overfitting, all possible 2-marker and 3-marker combinations were computed exhaustively. The results revealed that the top three 2-marker panels were *CLDN3* + *SNX6*, *CLDN3* + *PGRMC1*, and *AZGP1* + *SNX6*. This dual-gene signature achieved perfect discrimination,

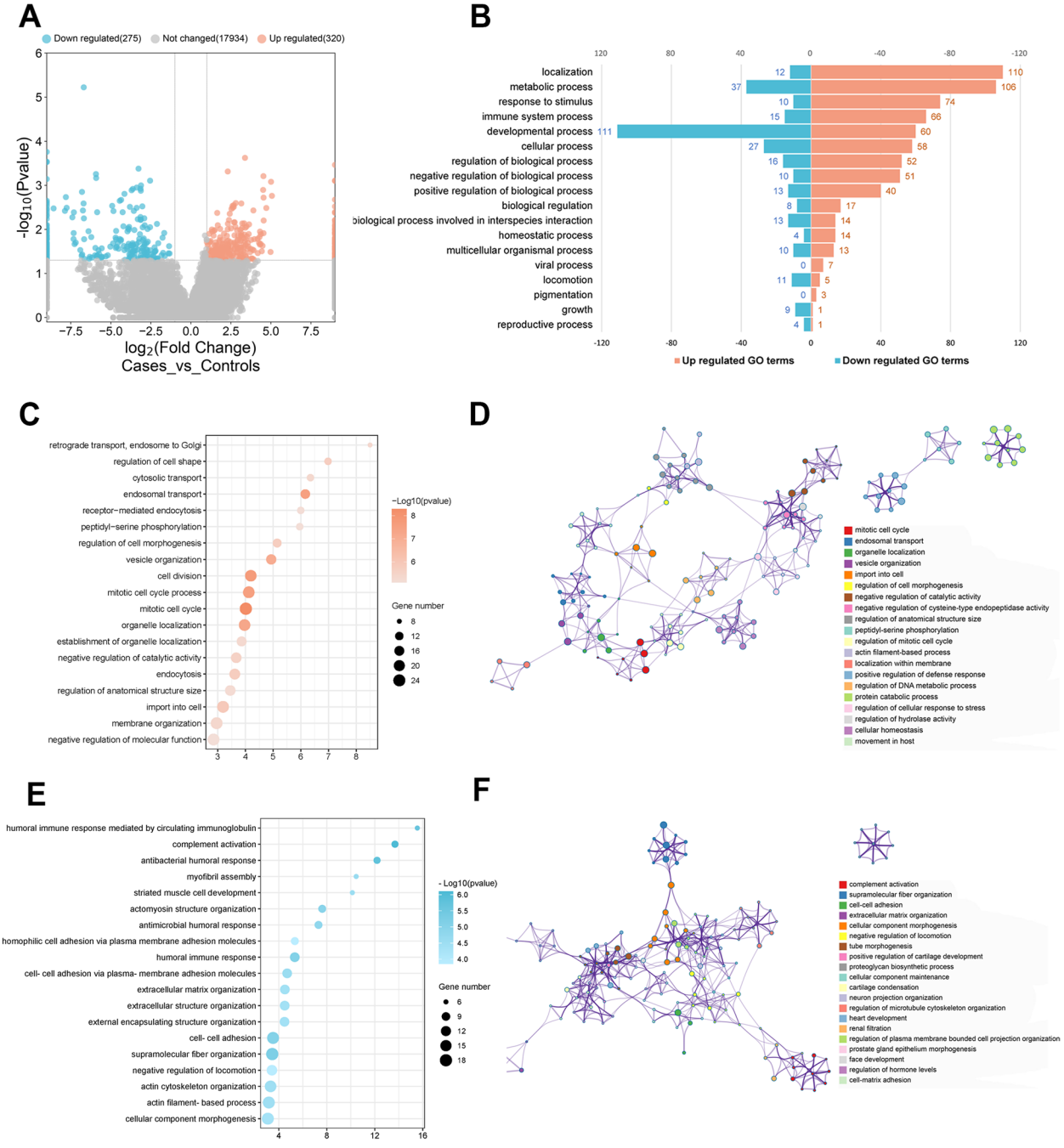

Fig. 2 Differential expression and functional enrichment analysis of salivary transcriptome in cases compared with controls. **A** Volcano plot indicates differentially expressed mRNAs in saliva of cases versus controls ($P < 0.05$, $|logFC| > 1.0$). Red dots represent up-regulated genes, blue dots represent down-regulated genes, and gray dots represent genes that were not differentially expressed. **B** The number and classes of all enriched GO biological process (BP) terms for up-regulated and down-regulated pathways. **C** Dot plot of the GO enrichment analysis shows the top 20 BP terms of up-regulated pathways. The horizontal axis represents the enrichment score, while the vertical axis represents the enriched pathway name. The color scale indicates different thresholds of the -log(*P*-value), and the size of the dot indicates the number of genes corresponding to each pathway. **D** Interaction network shows the relationships between the representative enriched up-regulated terms, where terms with a similarity > 0.3 are connected by edges. Each term is represented by a circle node, where its size is proportional to the number of genes under that term, and its color represent its cluster identity. The thickness of the edge represents the similarity score. **E** Dot plot of the GO enrichment analysis shows the top 20 BP terms of down-regulated pathways. **F** Interaction network shows the relationships between the representative enriched down-regulated terms, where terms with a similarity > 0.3 are connected by edges

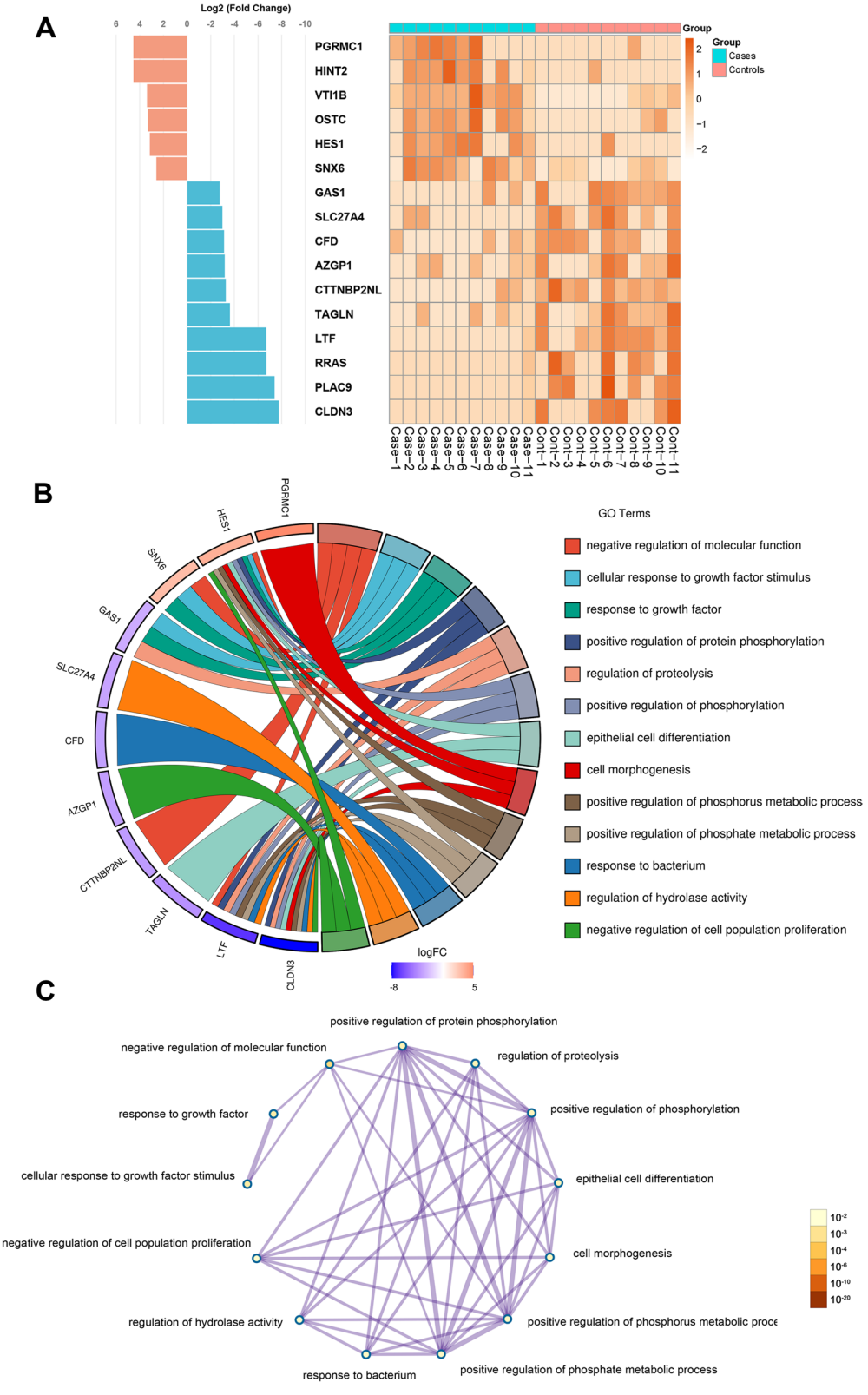

Fig. 3 (See legend on next page.)

(See figure on previous page.)

Fig. 3 Potential biomarker candidate genes and their functional enrichment analysis. **A** Differential expressions and fold changes of 16 candidate genes in saliva of cases and controls. The color in the heatmap represents the logarithmic FPKM of each gene. **B** The enriched GO terms in biological process for the candidate genes. The color of the gene label represents the log2-fold change of gene expressed in cases versus controls. **C** Interaction network shows the relationships between the enriched GO terms for candidate genes, where terms with a similarity > 0.3 are connected by edges. The thickness of the edge represents the similarity score. Each term is represented by a circle node, where its color represents its *P* value. The dark the color, the more statistically significant the node is

with an optimism-corrected AUC of 0.98–0.99. Notably, when the model complexity was increased to include 3-marker panels, the diagnostic metrics plateaued at 0.99. The addition of a third biomarker gene provided no incremental diagnostic benefit over the 2-marker panels. Guided by the statistical principle of parsimony, the 2-gene panel was identified as the diagnostic ceiling for OD, maximizing discriminatory power while minimizing assay complexity. The diagnostic performance of biomarker candidates was shown in Table 3.

Discussion

The precise epidemiological prevalence or incidence of OD, as a rare condition, remains unreported. A German study analyzed data from 1049 patients with temporomandibular disorders and identified nine cases of OD [14]. Despite our institution being the largest dental specialty hospital in North China, we collected only 11 OD patients over three years, highlighting the rarity of OD and the significant challenges it poses for clinical research. Most existing literature on OD consists of case reports, reviews, or expert opinions based on clinical experience. Limited studies suggest that OD is more prevalent in females than males [3, 7, 16, 46], with onset typically occurring between 20 and 80 years of age, peaking around 40–50 years [3, 5, 47]. In our cohort of 11 OD patients, comprising seven females and four males, ages ranged from 31 to 63 years, with an average age of 47, consistent with prior reports. Symptoms of OD typically manifest following routine dental treatments [3, 7, 8]. Various dental procedures, including restorative dentistry, endodontics, oral and maxillofacial surgery, orthodontics, and implantology, have been implicated in triggering OD [1]. In our study, 9 out of the 11 OD patients developed symptoms post-dental treatment, one was attributed to a stressful event, and one lacked a clear cause, aligning with the typical presentation of OD following dental interventions. Consequently, OD represents a latent threat that significantly impacts both practitioners and patients upon its manifestation. This study, therefore, aims to explore objective saliva biomarker candidates for the early detection of OD.

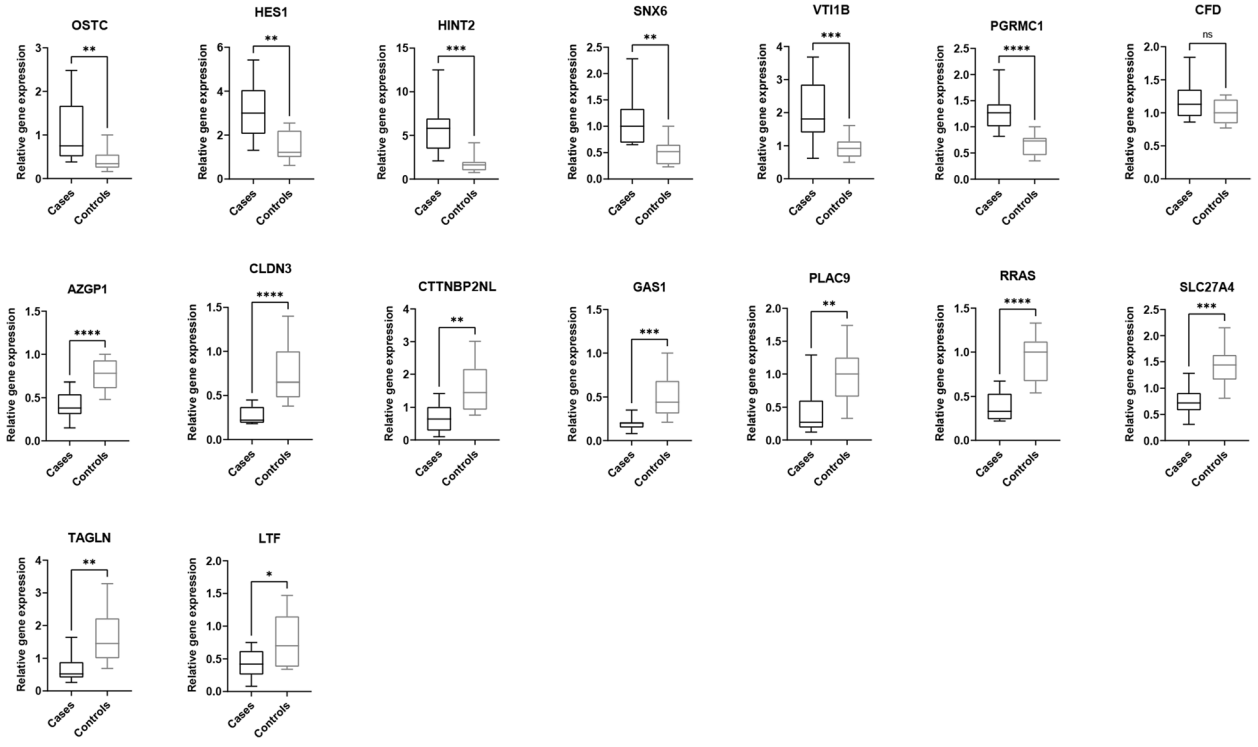

Fig. 4 Verification of 16 candidate genes through real-time PCR. *, $P < 0.05$; **, $P < 0.01$; ***, $P < 0.001$; ****, $P < 0.0001$; ns, not significant

Table 2 Association of salivary gene candidates with OD

	Model unadjusted		Model adjusted for age		Model adjusted for gender		Model adjusted for age and gender	
	OR (95% CI)	*p* Value	OR (95% CI)	*p* Value	OR (95% CI)	*p* Value	OR (95% CI)	*p* Value
AZGP1	53.24 (2.56, 1105.31)	**0.0102**	36.15 (2.49, 525.25)	**0.0086**	53.81 (2.35, 1232.01)	**0.0126**	42.06 (2.49, 709.45)	**0.0095**
CLDN3	35.91 (1.85, 697.65)	**0.0180**	26.45 (2.08, 336.81)	**0.0116**	25.59 (2.18, 299.86)	**0.0098**	21.29 (2.19, 206.65)	**0.0084**
SLC27A4	31.54 (2.33, 425.95)	**0.0094**	23.64 (2.21, 253.01)	**0.0089**	26.53 (2.40, 293.67)	**0.0075**	19.88 (2.23, 177.64)	**0.0074**
RRAS	28.03 (1.91, 411.58)	**0.0150**	23.71 (2.04, 275.48)	**0.0114**	20.38 (1.86, 223.18)	**0.0136**	22.05 (1.86, 261.45)	**0.0142**
GAS1	20.47 (1.97, 212.74)	**0.0115**	16.72 (1.86, 150.06)	**0.0119**	17.39 (1.93, 156.96)	**0.0109**	17.34 (1.84, 163.41)	**0.0127**
TAGLN	9.33 (1.67, 51.95)	**0.0108**	9.33 (1.75, 49.85)	**0.0090**	8.08 (1.63, 40.04)	**0.0105**	9.07 (1.67, 49.39)	**0.0108**
CTTNBP2NL	5.62 (1.24, 25.54)	**0.0255**	6.43 (1.21, 34.13)	**0.0288**	6.43 (1.32, 31.30)	**0.0211**	5.88 (1.30, 26.73)	**0.0217**
PLAC9	4.17 (1.40, 12.44)	**0.0104**	3.98 (1.38, 11.48)	**0.0105**	3.93 (1.38, 11.20)	**0.0105**	3.78 (1.36, 10.53)	**0.0110**
LTF	2.75 (0.89, 8.45)	0.0779	2.72 (0.89, 8.30)	0.0784	3.13 (0.90, 10.85)	0.0726	3.07 (0.87, 10.90)	0.0826
OSTC	0.19 (0.05, 0.76)	**0.0189**	0.21 (0.06, 0.78)	**0.0192**	0.21 (0.06, 0.77)	**0.0188**	0.24 (0.07, 0.80)	**0.0196**
HES1	0.14 (0.03, 0.66)	**0.0124**	0.16 (0.04, 0.68)	**0.0128**	0.16 (0.04, 0.64)	**0.0101**	0.17 (0.04, 0.66)	**0.0100**
HINT2	0.11 (0.02, 0.55)	**0.0074**	0.05 (0.00, 0.67)	**0.0231**	0.10 (0.02, 0.56)	**0.0085**	0.07 (0.01, 0.62)	**0.0171**
VTI1B	0.10 (0.02, 0.62)	**0.0135**	0.08 (0.01, 0.58)	**0.0126**	0.06 (0.01, 0.56)	**0.0136**	0.08 (0.01, 0.59)	**0.0132**
SNX6	0.07 (0.01, 0.69)	**0.0226**	0.07 (0.01, 0.60)	**0.0152**	0.08 (0.01, 0.61)	**0.0145**	0.08 (0.01, 0.61)	**0.0150**
PGRMC1	1.65e-03 (8.94e-06, 0.30)	**0.0160**	1.53e-03 (7.75e-06, 0.30)	**0.0162**	1.76e-03 (7.97e-06, 0.39)	**0.0212**	3.05e-03 (2.86e-05, 0.33)	**0.0150**

OD Occlusal dysesthesia, *OR* Odds ratios, *CI* Confidence interval. $p < 0.05$, Statistical differences are marked in bold. Genes with an OR > 1 suggests a protective effect, whereas an OR < 1 indicates increased risk, as the lower ΔCt values correspond to higher expression levels

Our findings reveal that saliva transcriptome sequencing identifies approximately five thousand genes in each saliva sample, consistent with previously reported data [24]. The proteins encoded by saliva mRNA are diverse, encompassing enzymes, transport proteins, transcription factors, membrane receptors, and cytoskeletal proteins, distributed across the nucleus, cytoplasm, and cell membrane. This underscores the notion that the transcriptomic signature of saliva may serve as an abridged mirror image of biological processes in the body, with the potential to unveil specific biomarkers for distal and systemic diseases. We observed significant up-regulation of *SNX6*, *VTI1B*, *HES1*, *HINT2*, *OSTC*, and *PGRMC1* in the saliva of OD patients, while *AZGP1*, *SLC27A4*, *TAGLN*, *LTF*, *CLDN3*, *CTTNBP2NL*, *GAS1*, *PLAC9*, and *RRAS* were significantly decreased. To ensure stabilized parameter estimation and robust confidence intervals despite the small sample size, Firth's penalized likelihood approach was employed. In all four constructed logistic models, high expression levels of *OSTC*, *HES1*, *HINT2*, *VTI1B*, *SNX6* and *PGRMC1*, as well as low expression of *AZGP1*, *CLDN3*, *SLC27A4*, *RRAS*, *GAS1*, *TAGLN*, *CTTNBP2NL*, and *PLAC9* in saliva, were consistently associated with an increased risk of OD, suggesting that these mRNAs in saliva may serve as potential biomarkers for the early identification of OD. Furthermore, all diagnostic panels were subjected to a 1000-resample Bootstrap optimism correction, to counteract overfitting issues in small sample sizes. The diagnostic utility results showed that three single-gene predictors, *CLDN3*, *RRAS*, and *PGRMC1*, achieved outstanding performance in discriminating OD from controls with optimism-corrected AUC > 0.90. Moreover, an exhaustive best-subset selection strategy demonstrated that the dual-gene panels (*CLDN3* + *SNX6*, *CLDN3* + *PGRMC1*, and *AZGP1* + *SNX6*) achieved perfect discrimination (corrected AUC > 0.98), and the integration of a third gene contributed no further diagnostic value. From a clinical translation perspective, a minimalist 2-gene diagnostic panel is highly favorable. The principle of parsimony ("less is more") is particularly relevant in molecular diagnostics. Compared to comprehensive multi-gene microarrays or sequencing panels, a 2-target qPCR assay significantly reduces turnaround time, simplifies interpretative algorithms, and minimizes financial costs for patients and healthcare systems.

Previous research indicates that these biomarker candidates are involved in various biological functions, with many being closely linked to the physiological and pathological functions of the nervous system. *CLDN3*, also known as the tight junction protein claudin-3, plays a pivotal role in maintaining the integrity of the blood-cerebrospinal fluid barrier in the choroid plexus [48]. Animals lacking *CLDN3* exhibit an accelerated onset and exacerbation of symptoms in experimental autoimmune encephalomyelitis [48]. *RRAS*, a member of the Ras

Table 3 Diagnostic performance of biomarker candidates for OD detection

Biomarker panel	Sensitivity	Specificity	Youden Index	Apparent AUC (95% CI)	Optimism-corrected AUC	*p* value
CLDN3	1.00	0.91	0.91	0.98 (0.90, 1.00)	0.91	**< 0.0001**
RRAS	1.00	0.82	0.82	0.97 (0.80, 1.00)	0.90	**< 0.0001**
PGRMC1	0.91	1.00	0.91	0.98 (0.93, 1.00)	0.90	**< 0.0001**
GAS1	1.00	0.82	0.82	0.96 (0.85, 1.00)	0.87	**< 0.0001**
AZGP1	1.00	0.73	0.73	0.94 (0.83, 1.00)	0.86	**< 0.0001**
HINT2	0.91	0.91	0.82	0.96 (0.87, 1.00)	0.86	**< 0.0001**
VTI1B	0.91	1.00	0.91	0.93 (0.78, 1.00)	0.85	**< 0.0001**
SLC27A4	1.00	0.73	0.73	0.92 (0.77, 1.00)	0.84	**0.0001**
SNX6	0.91	0.91	0.82	0.93 (0.79, 1.00)	0.83	**0.0002**
TAGLN	0.91	0.91	0.82	0.93 (0.79, 1.00)	0.81	**0.0014**
CTTNBP2NL	0.82	0.82	0.64	0.90 (0.74, 1.00)	0.77	**0.0079**
PLAC9	0.91	0.82	0.73	0.88 (0.71, 1.00)	0.76	**0.0129**
HES1	0.91	0.73	0.64	0.88 (0.72, 0.99)	0.75	**0.0157**
OSTC	0.91	0.73	0.64	0.88 (0.70, 0.99)	0.74	**0.0264**
LTF	1.00	0.45	0.45	0.76 (0.55, 0.94)	0.54	0.7508
CLDN3 + *SNX6*	1.00	1.00	1.00	1.00 (1.00, 1.00)	0.99	**< 0.0001**
CLDN3 + *PGRMC1*	1.00	1.00	1.00	1.00 (1.00, 1.00)	0.99	**< 0.0001**
AZGP1 + *SNX6*	1.00	1.00	1.00	1.00 (1.00, 1.00)	0.98	**< 0.0001**
CLDN3 + *RRAS* + *VTI1B*	1.00	1.00	1.00	1.00 (1.00, 1.00)	0.99	**< 0.0001**
CLDN3 + *PGRMC1* + *SNX6*	1.00	1.00	1.00	1.00 (1.00, 1.00)	0.99	**< 0.0001**
CLDN3 + *RRAS* + *SNX6*	1.00	1.00	1.00	1.00 (1.00, 1.00)	0.99	**< 0.0001**

OD Occlusal dysesthesia, *AUC* Area under the curve, *CI* Confidence interval. $p < 0.05$, Statistical differences are marked in bold. Optimism-Corrected AUC: The AUC calculated via 1000-resample Bootstrap iterations to rigorously adjust for overfitting in small sample sizes. Models are ranked by the Optimism-Corrected AUC

superfamily of small GTPases, is expressed by immune cells and has been shown to promote autoimmunity in experimental autoimmune encephalomyelitis [49]. Moreover, *RRAS* signaling has been identified as a pathological feature in Huntington's disease [50]. *PGRMC1*, also known as progesterone receptor membrane component 1, is widely distributed in the brain, with the highest expression observed in the limbic system [51, 52]. Numerous studies have highlighted the neuroprotective role of *PGRMC1*, which includes reducing levels of inflammatory factors in chronic neuroinflammatory conditions [53], alleviating antipsychotic drug-induced cognitive impairment [54], and contributing to the neuroprotective effects of progesterone in brain injury [55]. However, some studies also suggest that *PGRMC1* mediates the binding of amyloid-beta oligomers to synaptic puncta on neurons, thereby playing a crucial role in the pathological process of Alzheimer's disease [56]. *SNX6*, a sorting nexin protein that regulates endosomal trafficking, is critical for synaptic function in hippocampal neurons [57]. It interacts with the postsynaptic scaffold protein Homer1b/c to maintain dendritic spine density and AMPA receptor surface expression, thereby supporting spatial learning and memory [58]. In Alzheimer's disease, reduced *SNX6* levels contribute to increased BACE1 stability and amyloid-beta generation, linking it to pathological protein aggregation [59]. *AZGP1*, zinc-α2-glycoprotein, is expressed in hypothalamic neurons, particularly POMC neurons, where it enhances leptin signaling through JAK2-STAT3 phosphorylation to regulate energy homeostasis and metabolism [60]. In temporal lobe epilepsy, *AZGP1* expression is decreased in brain tissues, suggesting a potential role in neuronal excitability and seizure pathology [61]. It has also been identified as a potential serum biomarker in Alzheimer's disease, indicating its involvement in neurodegenerative processes [62]. *VTI1B* is a SNARE protein involved in late endosomal and lysosomal trafficking, essential for neurite outgrowth and synaptic receptor distribution in developing neurons [63]. In inflammatory pain, *VTI1B* promotes TRPV1 sensitization in sensory neurons, modulating thermal hypersensitivity without affecting basal nociception [64]. Loss of *VTI1B*, along with *VTI1A*, disrupts Golgi outpost formation and neurotrophic signaling, highlighting its role in neuronal development and disease-related trafficking defects [65]. The changes observed in salivary mRNAs in this study may be associated with CNS alterations in OD patients, thereby supporting the prevalent perspective that views OD as a psychiatric disorder characterized by somatic symptoms resulting from CNS dysfunction. Nonetheless, this study cannot conclusively determine the precise source of the

alterations in salivary mRNAs; hence, further research is warranted to elucidate the pathomechanisms underlying OD.

Limitations of this study include the small sample size. Despite the use of a highly rigorous and conservative statistical approach, these computational methods cannot substitute for external validation. Besides, the analysis was limited to adjustments for age and gender. Other potential residual confounding factors, such as psychosocial issues, medication use, and pain-related variables, cannot be excluded. Consequently, the strong diagnostic performance of the candidate gene markers for OD detection observed in this study still warrants cautious interpretation, and the findings should be viewed as exploratory rather than confirmatory. Given the rarity of OD, it is recommended that the academic community take advantage of multicenter collaborative research focusing on OD to acquire a larger sample size for further investigation, such as multiple time points in the progression of OD, subtype grouping, differential diagnostics, or multi-omics research.

Conclusion

This study provides the first delineation of the salivary transcriptomic profile of OD patients. While requiring external validation in larger cohorts and longitudinal studies, several salivary mRNA biomarker candidates associated with OD are exploratory identified.

Abbreviations

OD	Occlusal dysesthesia
PCR	Polymerase chain reaction
CNS	Central nervous system
mRNA	Messenger ribonucleic acid
FOT	Fraction of total
FPKM	Fragments per kilobase of exon model per million mapped reads
FDR	False discovery rate
GO	Gene ontology
BP	Biological process

Supplementary Information

The online version contains supplementary material available at https://doi.org/10.1186/s12903-026-09637-0.

Supplementary Material 1: Supplementary Fig. 1. STROBE flowchart of study participants.

Supplementary Material 2: Supplementary file 1. STROBE checklist of items that should be included in reports of cross-sectional case-control observational studies.

Supplementary Material 3: Supplementary Table 1. Primers for candidate genes and housekeeper gene used in real-time PCR.

Supplementary Material 4: Supplementary Table 2. Clinical characteristics of the OD participants.

Supplementary Material 5: Supplementary Table 3. Detailed information of salivary gene biomarker candidates for OD.

Acknowledgements

We would like to thank Shanghai Biotechnology Corporation for technical assistance and the support received from the National Key R&D Program of China, National Natural Science Foundation of China, and Beijing Natural Science Foundation.

Authors' contributions

Y. L. contributed to data acquisition, analysis, and interpretation, drafted manuscript. Y. K., Y. Z., J. L., S. M., and Y. X. contributed to data acquisition, analysis, and interpretation. C. Y., K. F. and Q. X. contributed to data interpretation, conception and critical revision of the manuscript. X. X. and Y. C. contributed to conception and design, drafted manuscript, critical revision of the manuscript. All authors read and approved the final manuscript.

Funding

This study was supported by the National Key R&D Program of China (2022YFE0118300), National Natural Science Foundation of China (No. 82170982, No.81970955), Beijing Natural Science Foundation (No. 7242171), and the Program for New Clinical Techniques and Therapies of Peking University School and Hospital of Stomatology (PKUSSNCT-26B09).

Data availability

The RNA sequencing data have been deposited in the NCBI Sequence Read Archive (SRA) database under the accession number SRP713095. The data can be accessed directly via the following link: https://www.ncbi.nlm.nih.gov/sra/SRP713095. Additional datasets analyzed in this research are available from the corresponding author upon reasonable request.

Declarations

Ethics approval and consent to participate

This project was approved by the Institutional Review Board of Peking University Hospital of Stomatology (PKUSSIRB-202054059; PKUSSIRB-202054059a), Beijing, China. All participants were provided with detailed information about the procedures, and written consent was obtained.

Consent for publication

Not applicable.

Competing interests

The authors declare no competing interests.

Author details

[1]Department of Prosthodontics, Peking University School and Hospital of Stomatology, National Center of Stomatology, National Clinical Research Center for Oral Diseases, National Engineering Research Center of Oral Biomaterials and Digital Medical Devices, Beijing Key Laboratory for Intelligent Biomanufacturing and Regeneration of Craniofacial Tissues, NHC Key Laboratory of Digital Stomatology, Beijing 100081, China
[2]Department of Preventive Dentistry, Peking University School and Hospital of Stomatology, National Center of Stomatology, National Clinical Research Center for Oral Diseases, National Engineering Research Center of Oral Biomaterials and Digital Medical Devices, Beijing Key Laboratory for Intelligent Biomanufacturing and Regeneration of Craniofacial Tissues, NHC Key Laboratory of Digital Stomatology, Beijing 100081, China
[3]Center for TMD and Orofacial Pain, Peking University School and Hospital of Stomatology, National Center of Stomatology, National Clinical Research Center for Oral Diseases, National Engineering Research Center of Oral Biomaterials and Digital Medical Devices, Beijing Key Laboratory for Intelligent Biomanufacturing and Regeneration of Craniofacial Tissues, NHC Key Laboratory of Digital Stomatology, Beijing 100081, China

Received: 23 July 2024 / Accepted: 12 August 2026
Published online: 20 August 2026

References

1. Tamaki K, Ishigaki S, Ogawa T, et al. Japan Prosthodontic Society position paper on "occlusal discomfort syndrome." J Prosthodont Res. 2016;60:156–66. https://doi.org/10.1016/j.jpor.2015.11.002.
2. Melis M, Zawawi KH. Occlusal dysesthesia: a topical narrative review. J Oral Rehabil. 2015;42:779–85. https://doi.org/10.1111/joor.12309.
3. Hara ES, Matsuka Y, Minakuchi H, et al. Occlusal dysesthesia: a qualitative systematic review of the epidemiology, aetiology and management. J Oral Rehabil. 2012;39:630–8. https://doi.org/10.1111/j.1365-2842.2012.02300.x.
4. Tinastepe N, Kucuk B, Oral K. Phantom bite: a case report and literature review. Cranio; 2015;33:228–31. https://doi.org/10.1179/2151090314Y.0000000002.
5. Toyofuku A, Kikuta T. Treatment of phantom bite syndrome with milnacipran - a case series. Neuropsychiatr Dis Treat. 2006;2:387–90. https://doi.org/10.2147/nedt.2006.2.3.387.
6. Jagger RG, Korszun A. Phantom bite revisited. Br Dent J. 2004;197:241–3. https://doi.org/10.1038/sj.bdj.4811613.
7. Watanabe M, Umezaki Y, Suzuki S, et al. Psychiatric comorbidities and psychopharmacological outcomes of phantom bite syndrome. J Psychosom Res. 2015;78:255–9. https://doi.org/10.1016/j.jpsychores.2014.11.010.
8. Ligas BB, Galang MT, BeGole EA, et al. Phantom bite: a survey of US orthodontists. Orthod Chic. 2011;12:38–47.
9. Reeves JN, Merrill RL. Diagnostic and treatment challenges in occlusal dysesthesia. J Calif Dent Assoc. 2007;35:198–207.
10. Sussex JM. Phantom bite. Br Dent J. 2004;197:660–660. https://doi.org/10.1038/sj.bdj.4811930.
11. Marbach JJ. Orofacial phantom pain: theory and phenomenology. J Am Dent Assoc. 1996;127:221–9. https://doi.org/10.14219/jada.archive.1996.0172.
12. Kelleher MG, Rasaratnam L, Djemal S. The paradoxes of phantom bite syndrome or occlusal dysaesthesia ('dysesthesia'). Dent Update. 2017;44:8–32. https://doi.org/10.12968/denu.2017.44.1.8.
13. Cao Y, Xie QF. Advance in research of occlusal dysesthesia. Zhonghua Kou Qiang Yi Xue Za Zhi. 2021;56:109–12. https://doi.org/10.3760/cma.j.cn112144-20200328-00175.
14. Imhoff B, Ahlers MO, Hugger A, et al. Occlusal dysesthesia-A clinical guideline. J Oral Rehabil. 2020;47:651–8. https://doi.org/10.1111/joor.12950.
15. Tsukiyama Y, Yamada A, Kuwatsuru R, Koyano K. Bio-psycho-social assessment of occlusal dysaesthesia patients. J Oral Rehabil. 2012;39:623–9. https://doi.org/10.1111/j.1365-2842.2012.02317.x.
16. Baba K, Aridome K, Haketa T, et al. Sensory perceptive and discriminative abilities of patients with occlusal dysesthesia. Nihon Hotetsu Shika Gakkai Zasshi. 2005;49:599–607. https://doi.org/10.2186/jjps.49.599.
17. Ono Y, Ishikawa Y, Munakata M, et al. Diagnosis of occlusal dysesthesia utilizing prefrontal hemodynamic activity with slight occlusal interference. Clin Exp Dent Res. 2016;2:129–35. https://doi.org/10.1002/cre2.32.
18. Roi A, Rusu LC, Roi CI, et al. A new approach for the diagnosis of systemic and oral diseases based on salivary biomolecules. Dis Markers. 2019;2019:1–11. https://doi.org/10.1155/2019/8761860.
19. Zhang CZ, Cheng XQ, Li JY, et al. Saliva in the diagnosis of diseases. Int J Oral Sci. 2016;8:133–7. https://doi.org/10.1038/ijos.2016.38.
20. Pfaffe T, Cooper-White J, Beyerlein P, et al. Diagnostic potential of saliva: current state and future applications. Clin Chem. 2011;57:675–87. https://doi.org/10.1373/clinchem.2010.153767.
21. Fabryova H, Celec P. On the origin and diagnostic use of salivary RNA. Oral Dis. 2014;20:146–52. https://doi.org/10.1111/odi.12098.
22. Wong DT. Salivaomics. J Am Dent Assoc. 2012;143:19S-24S. https://doi.org/10.14219/jada.archive.2012.0339.
23. Wang Z, Gerstein M, Snyder M. RNA-Seq: a revolutionary tool for transcriptomics. Nat Rev Genet. 2009;10:57–63. https://doi.org/10.1038/nrg2484.
24. Spielmann N, Ilsley D, Gu J, et al. The human salivary RNA transcriptome revealed by massively parallel sequencing. Clin Chem. 2012;58:1314–21. https://doi.org/10.1373/clinchem.2011.176941.
25. Li Y, Zhou X, St JM, Wong DT. RNA profiling of cell-free saliva using microarray technology. J Dent Res. 2004;83:199–203. https://doi.org/10.1177/154405910408300303.
26. Park NJ, Li Y, Yu T, et al. Characterization of RNA in saliva. Clin Chem. 2006;52:988–94. https://doi.org/10.1373/clinchem.2005.063206.
27. Hu S, Wang J, Meijer J, et al. Salivary proteomic and genomic biomarkers for primary Sjogren's syndrome. Arthritis Rheum. 2007;56:3588–600. https://doi.org/10.1002/art.22954.
28. Brinkmann O, Wong DT. Salivary transcriptome biomarkers in oral squamous cell cancer detection. Adv Clin Chem. 2011;55:21–34. https://doi.org/10.1016/b978-0-12-387042-1.00002-2.
29. Li Y, St JM, Zhou X, et al. Salivary transcriptome diagnostics for oral cancer detection. Clin Cancer Res. 2004;10:8442–50. https://doi.org/10.1158/1078-0432.CCR-04-1167.
30. Jeon YS, Cha JK, Choi SH, et al. Transcriptomic profiles and their correlations in saliva and gingival tissue biopsy samples from periodontitis and healthy patients. J Periodontal Implant Sci. 2020;50:313–26. https://doi.org/10.5051/jpis.1905460273.
31. Zhang L, Farrell JJ, Zhou H, et al. Salivary transcriptomic biomarkers for detection of resectable pancreatic cancer. Gastroenterology. 2010;138:949-957.e7. https://doi.org/10.1053/j.gastro.2009.11.010.
32. Li F, Yoshizawa JM, Kim KM, et al. Discovery and validation of salivary extracellular RNA biomarkers for noninvasive detection of gastric cancer. Clin Chem. 2018;64:1513–21. https://doi.org/10.1373/clinchem.2018.290569.
33. Zhang L, Xiao H, Karlan S, et al. Discovery and preclinical validation of salivary transcriptomic and proteomic biomarkers for the non-invasive detection of breast cancer. PLoS One. 2010;5:e15573. https://doi.org/10.1371/journal.pone.0015573.
34. Zhang L, Xiao H, Zhou H, et al. Development of transcriptomic biomarker signature in human saliva to detect lung cancer. Cell Mol Life Sci. 2012;69:3341–50. https://doi.org/10.1007/s00018-012-1027-0.
35. Lee YH, Kim JH, Zhou H, et al. Salivary transcriptomic biomarkers for detection of ovarian cancer: for serous papillary adenocarcinoma. J Mol Med (Berl). 2012;90:427–34. https://doi.org/10.1007/s00109-011-0829-0.
36. Yuan C, Ma Z, Tong P, et al. Peptidomic changes of saliva after non-surgical treatment of stage I/II generalized periodontitis. Oral Dis. 2022;28:1640–51. https://doi.org/10.1111/odi.13838.
37. Lee Y-H, Zhou H, Reiss JK, et al. Direct saliva transcriptome analysis. Clin Chem. 2011;57:1295–302. https://doi.org/10.1373/clinchem.2010.159210.
38. Palanisamy V, Wong DT. Transcriptomic analyses of saliva. Methods Mol Biol. 2010;666:43–51. https://doi.org/10.1007/978-1-60761-820-1_4.
39. Kim D, Langmead B, Salzberg SL. HISAT: a fast spliced aligner with low memory requirements. Nat Methods. 2015;12:357–60. https://doi.org/10.1038/nmeth.3317.
40. Mi H, Muruganujan A, Huang X, et al. Protocol update for large-scale genome and gene function analysis with the PANTHER classification system (v.14.0). Nat Protoc. 2019;14:703–21. https://doi.org/10.1038/s41596-019-0128-8.
41. Pertea M, Kim D, Pertea GM, et al. Transcript-level expression analysis of RNA-seq experiments with HISAT, StringTie and Ballgown. Nat Protoc. 2016;11:1650–67. https://doi.org/10.1038/nprot.2016.095.
42. Pertea M, Pertea GM, Antonescu CM, et al. StringTie enables improved reconstruction of a transcriptome from RNA-seq reads. Nat Biotechnol. 2015;33:290–5. https://doi.org/10.1038/nbt.3122.
43. Robinson MD, McCarthy DJ, Smyth GK. EdgeR: a Bioconductor package for differential expression analysis of digital gene expression data. Bioinformatics. 2010;26:139–40. https://doi.org/10.1093/bioinformatics/btp616.
44. Benjamini Y, Yekutieli D. The control of the false discovery rate in multiple testing under dependency. Ann Stat. 2001;29:1165–88.
45. Zhou Y, Zhou B, Pache L, et al. Metascape provides a biologist-oriented resource for the analysis of systems-level datasets. Nat Commun. 2019;10:1523. https://doi.org/10.1038/s41467-019-09234-6.
46. Shinohara Y, Umezaki Y, Minami I, et al. Comorbid depressive disorders and left-side dominant occlusal discomfort in patients with phantom bite syndrome. J Oral Rehabil. 2019;47:36–41. https://doi.org/10.1111/joor.12872.
47. Marbach JJ, Varoscak JR, Blank RT, Lund P. Phantom bite": classification and treatment. J Prosthet Dent. 1983;49:556–9. https://doi.org/10.1016/0022-3913(83)90322-0.
48. Kooij G, Kopplin K, Blasig R, et al. Disturbed function of the blood-cerebrospinal fluid barrier aggravates neuro-inflammation. Acta Neuropathol. 2014;128:267–77. https://doi.org/10.1007/s00401-013-1227-1.
49. Ray A, Basu S, Miller NM, et al. An increase in tolerogenic dendritic cell and natural regulatory T cell numbers during experimental autoimmune encephalomyelitis in *Rras-/-* mice results in attenuated disease. J Immunol. 2014;192:5109–17. https://doi.org/10.4049/jimmunol.1302254.
50. Miller JP, Yates BE, Al-Ramahi I, et al. A genome-scale RNA-interference screen identifies RRAS signaling as a pathologic feature of Huntington's disease. PLoS Genet. 2012;8:e1003042. https://doi.org/10.1371/journal.pgen.1003042.
51. Intlekofer KA, Petersen SL. Distribution of mRNAs encoding classical progestin receptor, progesterone membrane components 1 and 2, serpine mRNA binding protein 1, and progestin and ADIPOQ receptor family members 7 and 8 in rat forebrain. Neuroscience. 2011;172:55–65. https://doi.org/10.1016/j.neuroscience.2010.10.051.

52. Brinton RD, Thompson RF, Foy MR, et al. Progesterone receptors: form and function in brain. Front Neuroendocrinol. 2008;29:313–39. https://doi.org/10.1016/j.yfrne.2008.02.001.
53. Jo SL, Hong EJ. Progesterone Receptor Membrane Component 1 Regulates Cellular Stress Responses and Inflammatory Pathways in Chronic Neuroinflammatory Conditions. Antioxid Basel. 2024;13. https://doi.org/10.3390/antiox13020230.
54. Cao T, Wang L, Jiao S, et al. The involvement of PGRMC1 signaling in cognitive impairment induced by long-term clozapine treatment in rats. Neuropsychobiology. 2023;82:346–58. https://doi.org/10.1159/000533148.
55. Labombarda F, Gonzalez SL, Gonzalez DM, et al. Effects of injury and progesterone treatment on progesterone receptor and progesterone binding protein 25-Dx expression in the rat spinal cord. J Neurochem. 2003;87:902–13. https://doi.org/10.1046/j.1471-4159.2003.02055.x.
56. Izzo NJ, Xu J, Zeng C, et al. Alzheimer's therapeutics targeting amyloid beta 1–42 oligomers II: sigma-2/PGRMC1 receptors mediate Abeta 42 oligomer binding and synaptotoxicity. PLoS One. 2014;9:e111899. https://doi.org/10.1371/journal.pone.0111899.
57. Zhai J, Pan D, Jiang C, et al. Snx6-Mediated Subunit-Specific Secretory Trafficking of Ampa Receptors Regulates Synaptic Function and Plasticity. Commun Biol. 2025. https://doi.org/10.1038/s42003-025-09376-y.
58. Niu Y, Dai Z, Liu W, et al. Ablation of Snx6 Leads to Defects in Synaptic Function of Ca1 Pyramidal Neurons and Spatial Memory. Elife. 2017;6. https://doi.org/10.7554/elife.20991.
59. Li Q, Li X, Wang L, Zhang Y, Chen L. Mir-98-5P acts as a target for Alzheimer'S disease by regulating Aβ production through modulating Snx6 expression. J Mol Neurosci. 2016;60:413–20. https://doi.org/10.1007/s12031-016-0815-7.
60. Qiu S, Wu Q, Wang H, et al. Azgp1 in Pomc Neurons Modulates Energy Homeostasis and Metabolism through Leptin-Mediated Stat3 Phosphorylation. Nat Commun. 2024;15. https://doi.org/10.1038/s41467-024-47684-9.
61. Liu Y, Wang T, Liu X, Wei X, Xu T, Yin M, et al. Neuronal zinc-A2-glycoprotein is decreased in temporal lobe epilepsy in patients and rats. Neuroscience. 2017;357:56–66. https://doi.org/10.1016/j.neuroscience.2017.05.043.
62. Zhang X, Yu W, Cao X, Wang Y, Zhu C, Guan J. Identification of serum biomarkers in patients with Alzheimer's disease by 2D-Dige proteomics. Gerontology. 2022;68:686–98. https://doi.org/10.1159/000520961.
63. Kunwar AJ, Rickmann M, Backofen B, Browski SM, Rosenbusch J, Schöning S, et al. Lack of the endosomal snares Vti1a and Vti1B led to significant impairments in neuronal development. Proc Natl Acad Sci U S A. 2011;108:2575–80. https://doi.org/10.1073/pnas.1013891108.
64. Sondermann JR, Barry AM, Jahn O, Michel N, Abdelaziz R, Kügler S, et al. Vti1B promotes Trpv1 sensitization during inflammatory pain. Pain. 2018;160:508–27. https://doi.org/10.1097/j.pain.0000000000001418.
65. Bollmann C, Schöning S, Kotschnew K, Grosse J, Heitzig N, von Mollard GF. Primary Neurons Lacking the Snares Vti1a and Vti1B Show Altered Neuronal Development. Neural Dev. 2022;17. https://doi.org/10.1186/s13064-022-00168-2.

Publisher's Note

Springer Nature remains neutral with regard to jurisdictional claims in published maps and institutional affiliations.